Global and Planetary Change 210 (2022) 103756

Contents lists available at ScienceDirect

Global and Planetary Change

journal homepage: www.elsevier.com/locate/gloplacha

Climate-inferred distribution estimates of mid-to-late Pliocene hominins

Corentin Gibert [a,b,*,1], Anaïs Vignoles [a,1], Camille Contoux [c], William E. Banks [a,d], Doris Barboni [e], Jean-Renaud Boisserie [b,f], Olivier Chavasseau [b], Frédéric Fluteau [g], Franck Guy [b], Camille Noûs [h], Olga Otero [b], Pierre Sepulchre [c], Antoine Souron [a], Gilles Ramstein [c]

[a] University of Bordeaux, CNRS, MCC, PACEA, UMR 5199, Bâtiment B2, Allée Geoffroy St. Hilaire, CS 50023, 33600 Pessac, France
[b] Paléontologie, Evolution, Paléoécosystèmes, Paléoprimatologie (PALEVOPRIM), CNRS & Université de Poitiers, Poitiers, France
[c] Laboratoire des Sciences du Climat et de l'Environnement (LSCE), IPSL, Gif-sur-Yvette, France
[d] Biodiversity Institute, University of Kansas, 1345 Jayhawk Blvd, Lawrence, KS 66045, USA
[e] CEREGE, Aix Marseille Université, CNRS, IRD, INRAE, Aix-en-Provence, France
[f] Centre Français des Études Éthiopiennes, Ministère de l'Europe et des affaires étrangères & CNRS, PO BOX 5554, Addis Ababa, Ethiopia
[g] Institut de Physique du Globe de Paris (IPGP), Paris, France
[h] Laboratoire Cogitamus, Paris, France

ARTICLE INFO

Editor: Alan Haywood

Keywords:
Habitat suitability model
Niche modeling
Australopithecus
Africa
Pliocene
Dispersal

ABSTRACT

During the mid-to-late Pliocene (ca. 4–3 Ma), several hominin species were present in central Sahel, eastern and southern Africa. The potential for the discovery of hominin remains from this interval is limited by the availability of exposed Pliocene deposits and the ability to investigate them. As a result, most discoveries have been made in the Afar region of Ethiopia and in the Lake Turkana basin, thus unveiling only a portion of Pliocene hominins' probable geographical presence. In this study we provide a continental view of geographic areas potentially accessible to these hominins. To do so, we estimate the climatic envelope suitable for mid-to-late Pliocene hominin presence, using the earth system model IPSL-CM5A and the Maxent habitat suitability algorithm. Our analysis reveals high habitat suitability for these hominin species in semi-arid regions where annual thermal amplitude and mean annual precipitation are moderate, mostly corresponding to tropical xerophytic shrublands. Our habitat model estimates geographically continuous, suitable climatic conditions for hominins between central Sahel and northeastern Africa, but not between eastern and southern Africa. This discontinuity suggests that southern African and eastern African hominins were separated by an environmental barrier that could only be crossed during particularly favourable periods or by undertaking long-range dispersal over climatically hostile habitats. Under climate conditions of northern hemisphere summer at perihelion this climatic barrier is not present. In contrast, the Turkana basin, the Laetoli region, and a large part of southern Africa remain suitable for all precession angles, suggesting that these areas may have functioned as refugia. The constant presence of these stable areas combined with the periodic establishment of corridors for dispersion can potentially explain hominin diversity in eastern Africa.

1. Introduction

The mid-to-late Pliocene, ca. 4–3 million years ago (Ma), was a period of global warmth with atmospheric CO_2 concentrations around 400 ppm, smaller ice sheets, reduced desert areas compared to the present, and a global temperature 2–3 °C warmer than the preindustrial period (e.g. Salzmann et al., 2008; Haywood et al., 2020). Oxygen isotope ratios of benthic foraminifera and continental ice records show that this interval was climatically stable, with the exception of short-lived cold episodes around 3.6 Ma and 3.3 Ma (De Schepper et al., 2014; Lisiecki and Raymo, 2005). During this period, several hominin species appear to have coexisted and fossil occurences occur in three distinct geographic areas: central Sahel (*Australopithecus bahrelghazali*: Brunet et al., 1995, 1996; Lebatard et al., 2008), eastern Africa (*Au. anamensis, Au. afarensis*: Haile-Selassie et al., 2019; *Kenyanthropus platyops*: Leakey et al., 2001; *Au. deyiremeda*: Haile-Selassie et al., 2015)

* Corresponding author at: University of Bordeaux, CNRS, MCC, PACEA, UMR 5199, Bâtiment B2, Allée Geoffroy St. Hilaire, CS 50023, 33600 Pessac, France.
E-mail address: corentingibert@gmail.com (C. Gibert).
[1] Equally contributed, shared first-authorship.

https://doi.org/10.1016/j.gloplacha.2022.103756
Received 3 September 2021; Received in revised form 27 January 2022; Accepted 1 February 2022
Available online 4 February 2022

and southern Africa (*Au. prometheus*: Clarke and Kuman, 2019; *Au. africanus*: Dart, 1925; Herries et al., 2013*)*. These hominins thrived in C_3-C_4 mosaic habitats (Behrensmeyer and Reed, 2013), which are close to freshwater sources in the form of rivers (Curran and Haile-Selassie, 2016), springs and oases (Barboni et al., 2019), or lakes (paleo-lake Turkana: Feibel, 2011; Boës et al., 2019; paleo-lake Chad: Schuster et al., 2009; Lee-Thorp et al., 2012). They may have used technology, since the oldest recovered retouched pebble assemblage discovered near Lake Turkana is dated ca. 3.3–3.2 Ma (Harmand et al., 2015).

While their exploited microhabitats appear to have been mostly dominated by the presence of freshwater and some locally sustained trees, several authors propose that they could have coped with a variety of environments (within which similar microhabitats could occur), thus leading to the idea that the genus *Australopithecus* could have been eurytopic (Bonnefille et al., 2004; Behrensmeyer and Reed, 2013). Our ability, however, to observe and investigate hominin remains from this period is limited by the availability of exposed Pliocene deposits. As a result, most discoveries have been made in the Afar region of Ethiopia and the Lake Turkana Basin, thus representing only a portion of the probable Pliocene hominin geographic distribution. Here, we aim to provide a continental view of the geographic areas potentially accessible to these hominin populations. Reconstructing the presence of freshwater sources at reduced geographic scales is speculative for chronological intervals that have a resolution of hundreds of thousands of years and regions for which detailed paleotopography is unknown. However, sources of perennial freshwater and associated gallery vegetation can occur anywhere total annual precipitation exceeds 200–300 mm and topographic depressions or river channels exist (Quade et al., 2018). This is the case during the mid-Holocene and the Last Interglacial when surface drainage was reactivated in the Sahara (e.g. Coulthard et al., 2013; Skonieczny et al., 2015), as well as in areas where precipitation is lower than that threshold, but sustained by groundwater (e.g. present-day Ounianga lakes in northeastern Chad: Kröpelin et al., 2008). C_3-C_4 mosaic habitats, similar to those occupied by hominins, are ubiquitous in African savannah environments (Marston et al., 2019) for which woody cover depends on the frequency and intensity of individual rainfall events (Good and Caylor, 2011). Both are unknown for past intervals. Although there is a link between large-scale climate and hominid microhabitats, i.e., perennial freshwater sources enable the development of mosaic habitats, quantitative assessment of linkage is lacking.

We address these issues from a statistical point of view by employing climate envelope modeling methods to determine which large-scale climate variables are most appropriate for explaining known hominin occurrences between 4 Ma and 3 Ma and inferring their potential distributions. To do so, we employ a set of mid-to-late Pliocene climatic variables simulated with the earth system model IPSL-CM5A (Dufresne et al., 2013) to create a climatic envelope model that best matches the distribution of mid-to-late Pliocene hominin occurrences using the *kuenm* R package (Cobos et al., 2019), based on the Maxent algorithm (Phillips et al., 2006, 2017). Via this approach, we 1) evaluate the capacity of these methods to diagnose the appropriate areas for which we possess palaeobotanical and hominin data; 2) map potentially suitable areas currently free of paleontological remains and 3) employ a series of sensitivity experiments featuring extremes of precession-driven insolation changes for each season to investigate potential dispersal between our targeted geographic regions and potential refuge areas.

2. Methods

2.1. Climate model description and setup

We use the earth system model IPSL-CM5A to simulate late Pliocene climate. Atmospheric resolution of the model is 3.75° in longitude by 1.9° in latitude, with 39 vertical levels. Mean grid spacing of the ocean model is approximately 2°, while latitudinal resolution is refined to 0.5° near the equator and 1° in the Mediterranean Sea. This model has been widely used for the study of future and past climates (e.g. Dufresne et al., 2013; Kageyama et al., 2013; Contoux et al., 2012, 2015). The boundary conditions used to force the model follow the Pliocene Model Intercomparison Project phase 1 (PlioMIP1) guidelines described by Haywood et al. (2010). They have been adapted to the IPSL-CM5A model with a modified topography, smaller ice sheets, and atmospheric concentration of CO_2 fixed at 405 ppm (Contoux et al., 2012). The climate model uses PRISM3 boundary conditions designed to simulate the climate of the mid-Piacenzian (Haywood et al., 2011; Contoux et al., 2012). Benthic isotope ratios show that climate variability was low from 4 to 2.8 Ma except for two cold outbursts at 3.6 and 3.3 Ma (Lisiecki and Raymo, 2005; Tan et al., 2017, 2018). The Marine Isotope Stage (MIS) M2 (3.3 Ma) corresponds to the lowest level of reconstructed pCO_2 in the period covered in this study and the onset of a global glaciation leading to a 20 to 60 m sea-level drop. However, the pCO_2 reconstructions based on boron isotope, alkenone and benthic isotope $\delta^{18}O$ ratios depict strong variability (from 394 to 330 ppm *in* De La Vega et al., 2020; from 280 to 220 ppm *in* Tan et al., 2018) reflecting the difficulty to infer pCO_2 from data, whereas insolation changes and their consequences on Pliocene climate are easily computable. Given the pCO_2 stability at the scale of mid-to-late Pliocene (Tan et al., 2018), and the uncertainty of pCO2 reconstruction during the short MIS events, we extrapolate that PlioMIP boundary conditions are valids for the period between 4 and 3 Ma, which mostly corresponds to the Piacenzian. There exists a multitude of possible orbital configurations for any period that spans several hundred thousand years, but we can only use one set of orbital parameters per simulation since we conduct equilibrium climate simulations rather than transient ones. Because the primary goal of the PlioMIP simulation was to compare the climate of the mid-Piacenzian to the preindustrial, the choice made by the PlioMIP community was to use the present-day orbital configuration. This present-day configuration is one for which eccentricity is small. In other words, climate variability linked to precession, which is the main mode of climate variability during the Pliocene, is also small. Thus, we use it as a proxy for Pliocene 'mean' climate. This simulation (Pliocene 'mean' climate) has been extensively studied and compared to other climate models in the framework of PlioMIP1 (e.g. Haywood et al., 2010; Zhang et al., 2013). We also conducted four additional Pliocene experiments in order to capture an envelope of maximum climate variability during our target period. We do so using modified orbital parameters corresponding to the period of highest eccentricity (see appendix 1) with four different precession angles (one per simulation), corresponding to the Earth at perihelion at the Northern Hemisphere summer solstice (PlioMax June) and autumn equinox (PlioMax September), and the two opposites, at aphelion at Northern Hemisphere summer solstice (PlioMin June) and autumn equinox (PlioMin September). Orbital parameters were calculated using the Analyseries software (Paillard et al., 1996). Climatological means were calculated from the last 50 years of each simulation. Bias correction of the climate model output was obtained by using the climatic anomalies (temperature difference and percent change for precipitation, e.g. Hély et al., 2009) superimposed on Climate Research Unit climate observations at 0.5° by 0.5° (New et al., 2002). This is possible since the biases of a climate model are supposed to be stationary through different time periods (Krinner and Flanner, 2018). Our simulated climatic fields are thus downscaled from a resolution of 1.9° by 3.75° to 0.5° by 0.5°.

2.2. Vegetation model description and setup

We employed the BIOME4 model (Kaplan et al., 2003) to calculate vegetation in equilibrium with the Pliocene mean climate and the four orbital Pliocene climates. To do so, we calculated climate anomalies between each Pliocene experiment and the preindustrial control experiment (temperature difference and percentage of change for precipitation and clouds, e.g. Hély et al., 2009) interpolated at 0.5°x0.5°. The anomalies were then added to the 0.5°x0.5° gridded data from the

Climate Research Unit (New et al., 2002). The model BIOME4 calculates vegetation types in equilibrium with climate model outputs (monthly mean precipitation, air surface temperature, cloud cover and absolute annual minimum air surface temperature). Atmospheric CO_2 concentration was fixed at 405 ppm (PlioMIP value) and soil characteristics kept at present-day values.

In BIOME4, biomes are assigned according to which plant functional types (PFT) are dominant, as well as the productivity and leaf area index (LAI) of each PFT (Harrison and Prentice, 2003; Kaplan et al., 2003). For example, when the productivity on one grid cell is dominated by the the tropical raingreen tree PFT, followed by the C_4 tropical grass and the woody desert PFT, the grid cell will be associated with tropical xerophytic shrubland biome if the LAI of the tropical raingreen tree PFT is <4 and to the tropical savannah biome if the LAI of tropical raingreen tree PFT is >4.

2.3. Hominin occurrence data

Predictive architectures used to estimate ecological niches or climatic envelopes rely, in part, upon the geographic coordinates (longitude and latitude) of locations where the target population has been observed. In this study, the occurrence data are the locations where fossil hominins dated from ca. 4–3 Ma have been recovered. This choice was made for several reasons. First, our climate model is representative of Piacenzian climate (ca. 3.6—2.8 Ma). This corresponds to the chronological interval to which *Au. afarensis* has been dated. Climatic envelope modeling is performed typically at the species level. However, the diversity of Australopithecus species is poorly constrained as some species, and even genera, are controversial *(Au. bahrelghazali, Au. prometheus, K. platyops*). The intra-specific and inter-specific variability of Australopithecus species is also poorly understood, such that with the recent discovery of the first complete cranium of *Au. anamensis* (Haile-Selassie et al., 2019) remains previously assigned to *Au. afarensis* were reclassified as *Au. anamensis*. Given the taxonomic uncertainty of many *Australopithecus* remains, and considering that the genus provides a working framework, we chose to simulate the climatic envelope suitable for the ensemble of Pliocene *Australopithecus* species, as well as *Kenyanthropus*. This approach is justified by the review of *Australopithecus* paleoenvironments carried out by Behrensmeyer and Reed (2013) demonstrating that these hominins are all associated with similar environments, thus suggesting that their climatic envelopes were likely similar. We excluded the more primitive *Ardipithecus*, which is older than 4 Ma, as well as *Australopithecus* species that are clearly Pleistocene in age (*Au. garhi* and *Au. sediba*) since climatic deterioration due to the Northern Hemisphere Glaciation was already well established by that time (e.g. Tan et al., 2018).

In order to have independent training and test data sets and to limit spatial auto-correlation, we eliminated multiple occurrences such that a grid cell (0.5° by 0.5°) only contained a single occurrence point (see below). As a result, we have only 18 occurrence points (Table 1) despite the fact that more than 18 paleontological sites exist. Most of these localities are tightly clustered, especially in the Awash Valley and the Turkana Basin.

2.4. Maxent climate envelope model and kuenm R package descriptions and set-up

We use the term “climatic envelope modelling” to describe our approach. This term expresses the idea that “a multivariate space of climatic variables best matching the observed species' distribution is being estimated” (Araújo and Peterson, 2012). It does not imply a direct link with Hutchinson's theory of ecological niches, as is the case with the term “ecological niche modeling”. In this study, we assume that aspects of climate determine, at least in part, species distributions, and we do not interpret the resulting predictions within a strict ecological niche framework. The output from the Maxent model is termed habitat suitability index. This term of habitat should not be interpreted in the sense of microhabitat because the climatic data that we provide Maxent are at a large scale of 0.5° (i.e. roughly 2500 km^2). The term habitat suitability index should be understood as a measure of how suitable the large-scale environment was to the targeted African Pliocene hominins.

Table 1
Hominin occurrence points used in this study. The sites of Assa Issie (*Au. anamensis*), Aramis (*Ardipithecus* and *Au. anamensis*), Maka and Belohdelie (*Au. afarensis*) and Bouri (*Au. garhi*) all fall in the grid cell ‘Middle Awash’ because of their geographic proximity.

Occurrence point	Lon (°)	Lat (°)	Age (Ma)	Age reference
Koro-Toro	19.0	16.0	3.5—3	Brunet et al., 1995; Lebatard et al., 2008
Woranso-Mille	40.5	11.5	3.8—3.3	Deino et al., 2010; Haile-Selassie et al., 2012, 2015; Saylor et al., 2019
Hadar & Dikika	40.5	11.0	3.5—2.9	Behrensmeyer and Reed, 2013; Alemseged et al., 2006
Middle Awash	40.5	10.5	4.2—3.4	White et al., 1993, 2006a; Renne et al., 1999
Galili	40.5	9.5	4.5—3.5	Kullmer et al., 2008
Usno	36.0	5.5	ca. 3.4	White et al., 2006b
Shungura	36.0	5.0	3.5—3	Brown et al., 2013
Fejej	36.5	4.5	4—3.6	Kappelman et al., 1996; Fleagle et al., 1991
Koobi Fora	35.5	4.0	4.3—2.7	Brown et al., 2013
Allia Bay	36.5	4.0	4.1—3.8	Behrensmeyer and Reed, 2013
Lomekwi	36.5	3.5	3.5	Leakey et al., 2001
Lothagam	36.0	3.0	ca. 3.5	Leakey and Walker, 2003
Kanapoi	36.0	2.5	4.2—4	Leakey et al., 1998; Ward et al., 2013
Kantis	36.5	−1.5	3.5—3.4	Mbua et al., 2016
Laetoli	35.0	−3.5	3.8—3.4	Su and Harrison, 2008
Makapansgat	29.0	−24.0	3.4—2.6	Herries et al., 2013
Sterkfontein (member 2)	27.5	−26.0	3.6—3	Bruxelles et al., 2019
Taung	24.5	−27.5	3—2.6	Herries et al., 2013

To model the climatic envelope, we use the Maxent algorithm (Phillips et al., 2006, 2017; Phillips and Dudík, 2008), which has shown to perform well compared to other correlative predictive architectures, especially when relying on limited occurrences datasets (e.g. Phillips et al., 2006; Elith et al., 2006; Hernandez et al., 2006). Maxent requires the geographic location of sites where the target species have been observed (i.e., fossil localities) and geographically continuous environmental variables over the region of interest, which are derived from the climate model described above.

Maxent is based on the maximum entropy principle such that the estimated probability distribution is constrained by climatic characteristic associated with the known occurrence localities while it avoids assumptions not supported by the data. Maxent is not a classical presence-absence modeling method, but rather a presence-background method as real absences are not known and cannot be taken into account during the sampling of environmental variables (Guisan et al., 2017). This approach to background sampling makes Maxent suitable for making distributional predictions based on paleontological data. Maxent will compare the probability distribution associated with presence occurrences with the one associated with background points randomly sampled in the environment. The area over which this comparison will be done (i.e. the calibration area) has a great influence on model performance. Its size should be neither too small or too large (e.g. VanDerWal et al., 2009), and should be biologically meaningful to ensure that the background points represent the environmental conditions accessible to the species (Anderson and Raza, 2010; Barve et al., 2011). The calibration area encompassing all occurrences points and used in Maxent models can be found in Appendix 1. Maxent, however, is known to be sensitive to model settings (e.g. parameterization, number of variables) that affect model complexity (Warren and Seifert, 2011;

Peterson et al., 2018). The more complex a model is, the more likely it will be overfitted. The more overfitted a model is, the more it will struggle to extrapolate suitable habitats outside areas where occurrences are already known (Peterson et al., 2007).

In order to address this sensitivity and select the optimal parameterization, we employed the *kuenm* R package (Cobos et al., 2019) to produce and evaluate candidate models, as well as to perform final evaluations of the best models. We performed model calibration by testing the performance of 2210 candidate models. We produced these models using 26 distinct variable sets, made up of all unique combinations of two or more of the five least correlated climatic variables from the Pliocene 'mean' climate simulation descibed below. The candidate models also employed one of 17 regularization multipliers (0.1–1 at intervals of 0.1, 2–6 at intervals of 1, as well as 8 and 10), and five feature classes or feature class combinations (q, qp, lp, lq, lqp; l = linear, q = quadratic, p = product). We based our evaluations of the candidate models' performance by first evaluating significance and predictive power using partial ROC (500 iterations, and 50% of data for bootstrapping; Peterson et al., 2008) and omission rate metrics. We then evaluated model complexity using the Akaike Information Criterion for small sample sizes (AICc) (Warren and Seifert, 2011). We retained model parameterizations that resulted in statistically significant models, resulted in omission rates lower than 5%, and ΔAICc values less than two. The parameters of these retained models were used to create final models with 10 replicates by bootstrapping. The complete *kuenm* R script that used the Pliocene 'mean' climate model is provided as an Rmarkdown document in Appendix 2. The final model was projected onto the sets of environmental conditions for each of the four precession angle configurations. During the process of model projection, we allowed free extrapolation given the response curves (i.e., response curves not truncated for at least two variables) observed during model calibration. In order to consider, the risks associated with strict extrapolation and to prevent misinterpretation of transferred areas with non-analogous conditions, we employed the mobility-oriented parity (MOP) metric (Owens et al., 2013). Following the approach suggested by Pearson et al. (2006) for small sample sizes, the simulated climatic envelope represents "regions that have similar environmental conditions to where the species is known to occur, and not as predicting actual limits to the range of a species", given that absence of proof is not the proof of absence (see Discussion). The lower threshold for hominin presence was set to the value of the lowesthabitat suitability index (fixed sensitivity; Peterson et al., 2011: p.119) score amongst the occurrence points.

The five variables used for predicting the envelope model are representative of mean climate and seasonality: Warmest Month Temperature (WMT), Coldest Month Temperature (CMT), Temperature Difference between the warmest and the coldest months (DT), Mean Annual Precipitation (MAP), and Driest Month Precipitation (DMP). Mean Annual Temperature (MAT), Wettest Month Precipitation (WMP), Precipitation Difference between the wettest and the driest months (DP) and Net Primary Productivity (NPP) were excluded from the final analysis following the recommendations of, e.g. Merow et al. (2013) because they contributed only marginally to the definition of the climatic envelope and were highly correlated to the employed variables. The absence of vegetation variables (e.g. NPP) in the candidate models can be explained by the fact that we did not used a dynamic global vegetation model (DGVM), but we prescribed biome and computed NPP from climatic variables without feedback on climate. The candidate models used to build the final model do not necessarily include all of the five selected variables as the model overfits fossil occurrence data with increasing number of predictors (Guisan et al., 2017).

Given the chronological uncertainty associated with hominin fossil contexts and the temporal span of the targeted period, we cannot associate specific fossils or groups of fossils with a particular orbital configuration. The most conservative choice is to use the least extreme orbital configuration—Pliocene 'mean' climate—to estimate a climatic envelope. With this configuration, eccentricity is small thereby favoring lower seasonality and lower climatic variability linked to precession. To detect suitable areas that remained stable across the four precession configurations (i.e. refugia), we thresholded the final model and each projection by reclassifying as non-suitable (i.e. 0) all grid cells with suitability scores lower than the lowest value amongst the occurrence points. Next, suitability scores were grouped into three equal categories (low-, mid- and high-suitability areas) to facilitate the reading of the models' geographic projections and prevent direct interpretations of suitability values.

$$e.g. Low\ suitability\ areas\ range\ from min(suitability)\ to\ \left(min(suitability) + \frac{max(suitability) - min(suitability)}{3}\right)$$

Finally, a binary model was computed by reclassifying all suitable grid cells as one and non-suitable cells as zero. We then compared the four obtained binary predictions with the main Pliocene 'mean' climate model to reveal temporally stable areas of suitability.

2.5. Temporal and spatial sampling sensitivity tests

In order to test the sensitivity of our climatic envelope model to the chosen temporal window with respect to occurence sampling, we replicated the approach described above by removing the oldest and most recent Australipthecus taxa from the dataset (i.e. *A. anamensis*, A. africanus, *A. prometheus*). The localities, Lomekwi, Kanapoi, Makapansgat, Sterkfontein and Taung, are removed from model computation, resulting in the loss of all South African occurrences. The map of habitat suitability corresponding to this sensitivity test is available in Appendix 1. As recommended for small occurrence datasets (Pearson et al., 2006; Shcheglovitova and Anderson, 2013), we used a delete-one jackknife approach (or leave one out approach) to evaluate the influence of individual occurence on predictive variability. We removed one locality from the dataset, computed the model with $n - 1$ localities in *kuenm* and repeated this process until every locality have been removed once (i.e. n separate models for n observed localities). The n projections of these n models, as well as a consensus of all projections, are available in Appendix 1.

3. Results

3.1. Climate model validation

First, we assess the validity of the climate model at hominin sites by comparing paleoenvironmental reconstructions to the biome simulated with the BIOME4 model using IPSL-CM5A climate variables (see Supplementary Material). Vegetation reconstructions at hominin sites describe a seasonal, dry mosaic of woodland, shrubland and grassland (Behrensmeyer and Reed, 2013 and references therein), with small-scale more mesic environments sustained by local water resources (e.g. microhabitats sustained by rivers, lakes and springs; see Barboni et al., 2019). The BIOME4 model indicates tropical xerophytic shrubland,

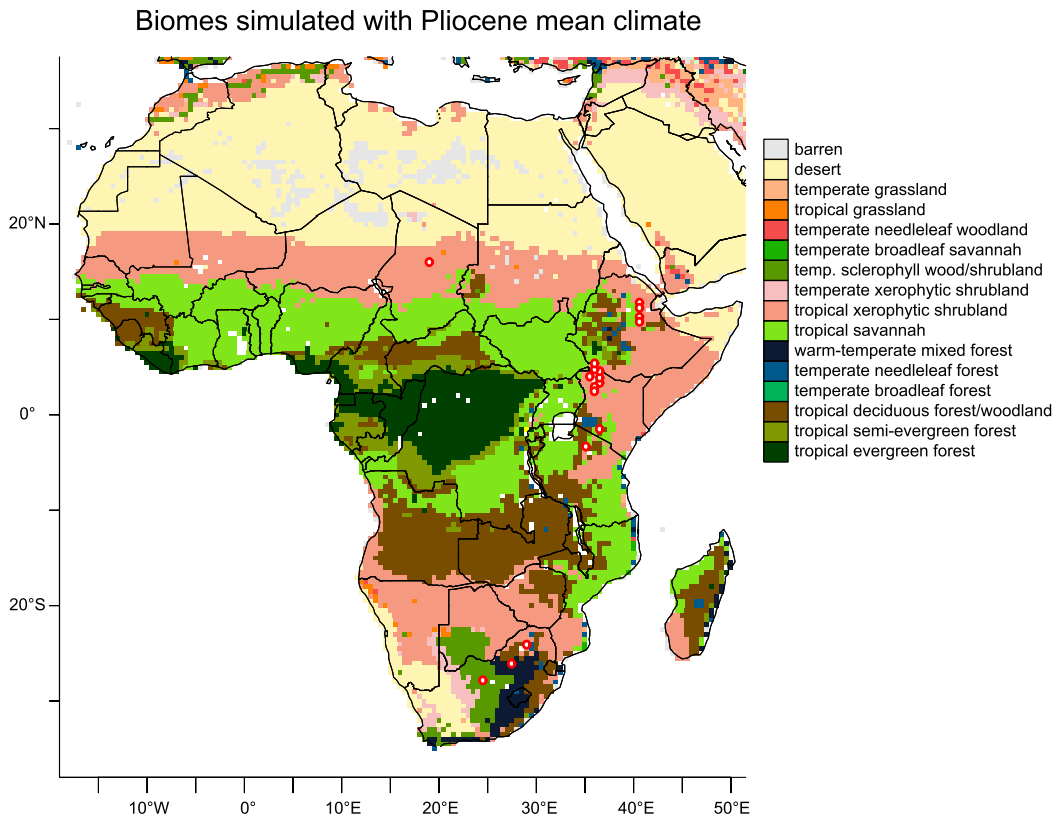

Fig. 1. Vegetation simulated with BIOME4 for the Pliocene mean climate. Red circles are the 18 hominin occurrence points. (For interpretation of the references to colour in this figure legend, the reader is referred to the web version of this article.)

tropical savannah, or tropical deciduous woodland at 16 of the 18 hominin localities (Fig. 1, see also Methods). In the BIOME4 model, productivity is higher in tropical deciduous woodland (Kantis locality) than in tropical savannah (Usno and Laetoli localities), and in tropical savannah than in tropical xerophytic shrubland (e.g. Awash Valley, Koro-Toro locality), but the same plant functional types are present in these three biomes. These biomes describe a mix of tropical raingreen trees, C_4 tropical grass, and woody desert plant functional types (C_3 and C_4) that correspond to a warm, seasonally dry climate, which is in good agreement with the mosaic of woodland, bushland and grassland inferred from vegetation reconstructions, although local-scale water sources are invisible to the model. Beside the hominin sites, paleovegetation reconstructions are available in few sites along the Atlantic coasts of Namibia and Nigeria, the coasts of Somalia, Sudan and Morocco (Salzmann et al., 2013). Tropical evergreen forests modelled by BIOME4 in central Africa, as well as the xerophytic shrubland in Morocco match fossil remains. However, in Namibia, Somalia and Sudan, modelled biomes are drier than the reconstructed paleovegetation (e.g. desert is modelled when xerophytic shrubland remains are discovered). These deviations toward drier conditions between modelled vegetation and fossil remains could be linked with the absence of local-scale water sources like large lake and soil in the climate model. Sensitivity analysis based on the presence/absence of lake in northern and central Africa (Pound et al., 2014; Dowsett et al., 2016) demonstrate that the presence of large lake can increase mean and seasonal precipitation over mid-latitudes of Africa, promoting the development of wetter biomes.

3.2. Hominin climatic envelope estimations and robustness

At a regional scale, the highest habitat suitability areas reconstructed by the climatic envelope model are located in tropical eastern Africa, except over eastern Somalia and western Ethiopia (Fig. 2). The Turkana Basin, areas west of Lake Victoria, as well as a region covering southern Somalia, eastern Kenya and northern Tanzania (including Laetoli and coastal regions, hereafter called the SKT region), and finally western Eritrea, northern Somalia-Djibouti and eastern Ethiopia (including the Awash valley) are the most climatically suitable regions for *Australopithecus*. Three other regions show reasonable habitat suitability indices. The first is a latitudinal corridor at ca. 15°N, covering Africa from the Atlantic coast to the Red Sea, at roughly the latitude of Lake Chad. This Sahelian corridor suggests a probable continuity of environmental conditions between the Awash valley and the Lake Chad region, with the potential for population dispersals within this corridor. The second area of interest is located in South Africa, southwestern Angola, Botswana, non-coastal Namibia, southern Mozambique, and southeastern Zimbabwe. This area is not connected to eastern Africa in our model, suggesting that population dispersals to or from this southern African area would not have been possible under mean Pliocene climate conditions. The last area is located on the African Mediterranean coast, including the locality of Ain Boucherit, where no Pliocene hominins have been recovered to date, but where stone artefacts and cut-marked bones dating to ca. 2.4 Ma are documented (Sahnouni et al., 2018). Our geographic coverage also includes southern regions of Eurasia (e.g. Yemen, Israel, Jordan, parts of southern Europe) for which habitat suitability attains values suggesting that mid-to-late Pliocene hominins could have survived in these regions if they had been accessible. After *kuenm* calibration process, the final model meeting significance and complexity requirements (of 2210 candidate models) is based on two of the five available variables: the temperature difference between the warmest and the coldest month (DT) and mean annual precipitation (MAP). All hominin occurrences are located in regions where annual

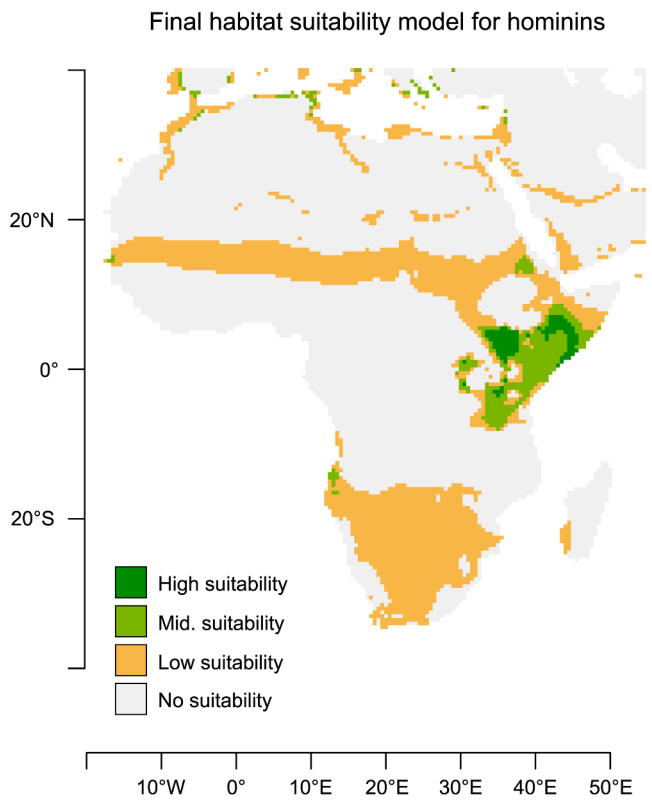

Fig. 2. Habitat suitability index for hominins under the Pliocene mean climate scenario. All values above the lowest presence threshold are shown (see Methods). Low suitability regroups cells with habitat suitability values ranging from 0.08–0.36; middle suitability range from 0.36–0.63; and high suitability is assigned to cells with values over 0.63. The final *kuenm* model is based on the DT and MAP variables.

precipitation is below 800 mm/yr with a marked dry season and limited annual thermal amplitude (up to 15 °C; Fig. 3) inside semi-arid zones (BS in the Köppen-Geiger classification, Peel et al., 2007).

Sensitivity tests on the occurrence data (i.e., leave one out approach) reveal that habitat suitability in the Sahelian corridor is not governed by a single locality, not even Koro-Toro located in central Sahel, while the suitable area in northern Africa is a result of climatic similarities to occurrence points located in eastern Africa (e.g. the Middle Awash) or in southern Africa (e.g. Taung; see Suppl. Fig. 1). The Allia Bay locality in Kenya has the strongest influence on suitability scores in the Sahelian corridor, but even its removal is insufficient to make this pattern disappear. The consensus map (see Suppl. Fig. 1), which combines all the sensitivity tests, demonstrates the robustness of the depicted pattern for hominins in Pliocene 'mean' climate (Fig. 2) by preserving the three main areas of suitable habitats (i.e. eastern, southern Africa, and the Sahelian corridor).

The sensitivity test conducted via temporal sampling (i.e. the removal of youngest and oldest species; see Suppl. Fig. 2) demonstrates the robustness of the climate envelope modelled with all selected occurrences (Fig. 2). We performed this test without the three localities from South Africa and nevertheless the same areas remain suitable for hominins. The main differences between this sensitivity test and the main model are the absolute suitability values in suitable areas. In southern Africa, the eastern coast depicts middle and high suitability in the sensitivity test while in the main model these areas are associated with low suitability scores. In northern Africa and the European Mediterranean coast, suitability values are higher in the test, while conversely the areas of middle and high suitability in eastern Africa are more geographically limited than in the main model.

Our results show that eastern and southern Africa were not connected, with respect to suitability, under Pliocene mean conditions. However, we know that *Australopithecus* was present both in eastern and southern Africa, indicating that either: 1) climate variability allowed them to cross this environmental barrier; or 2) they were able to reach/occupy both regions because their niche was in fact broader or because they attempted long-range dispersal across climatically unsuitable areas. In an effort to evaluate the first hypothesis, we further examined potential geographic variability of suitable areas for mid-to-late Pliocene hominins caused by orbital precession changes.

3.3. Orbitally driven climate variability and potential dispersals

We projected the climatic envelope estimated from Pliocene mean climate conditions onto four Pliocene climate scenarios simulated with summer and autumn insolation maxima and minima (Figure 4, Suppl. Fig. 3-6). This provides examples of the potential ability of Pliocene hominins to disperse.

geographically during specific climate scenarios driven by orbital precession variability—dispersals that would not necessitate them changing the environmental conditions they exploited.

During periods of boreal summer or autumn insolation maxima (PlioMax June simulation and PlioMax September simulation, respectively), the Afar region and a large portion of eastern Africa are unsuitable, except for the Turkana region and the SKT region (including the Laetoli and coastal regions) (Fig. 4). During these periods, the tropical rain belt is located further north. The Sahelian band of suitability is shifted north of Koro-Toro (Suppl. Fig. 5) into the present-day Sahara for PlioMax September, and it is totally absent for PlioMax June. There remains a large unsuitable area between Laetoli (the southernmost eastern African site) and Makapansgat (the northernmost southern African site) for three of the configurations. However, in the PlioMax June projection (i.e. boreal summer maxima), a continuous zone of middle and high climatic suitability between eastern and southern Africa emerges (Fig. 4, bottom left), which would have allowed hominin dispersal to/from the south. Variations in precession angle could therefore be a potential factor controlling the emergence of corridors permitting the dispersion of ancient hominins between eastern and southern Africa along the Kingdon line (Kingdon, 2003; Joordens et al., 2019). During periods of boreal summer insolation minima (Fig. 4, top left, PlioMin June), the habitat suitability indices becomes high in the northern part of the African rift, particularly in the Ethiopian highlands, down to the Baringo locality and also extend down to Laetoli through the SKT region. Suitability in the Sahelian band increases strongly and shifts southward following the tropical rain belt. Three areas remain above the lowest presence threshold for all orbital configurations and can therefore be considered as true core areas or refugia (Fig. 5) —the Turkana Basin, the SKT region, and a vast portion of southern Africa. To the contrary, the Sahelian band and the Awash Valley remain suitable in some, but not all, of the four climate scenarios.

4. Discussion

4.1. Australopithecus in semi-arid climate

From the late Miocene onwards, early hominins were not found in sites sampling densely forested environments nor shadowless plains, but instead are known from more or less wooded, mosaic habitats (see Sponheimer, 2013). The earliest known hominin, *Sahelanthropus tchadensis*, lived in a Sahelian-like mosaic landscape close to lake settings (Vignaud et al., 2002; Le Fur et al., 2009; Blondel et al., 2010; Novello et al., 2017). The early Pliocene hominins *Ardipithecus ramidus* and *Ardipithecus kadabba* are also thought to have lived in an open, wooded savannah biome (Levin et al., 2008; White et al., 1994, 2009; Cerling et al., 2011), within which they occupied localized forested microhabitats sustained by springs (WoldeGabriel et al., 2009; Barboni

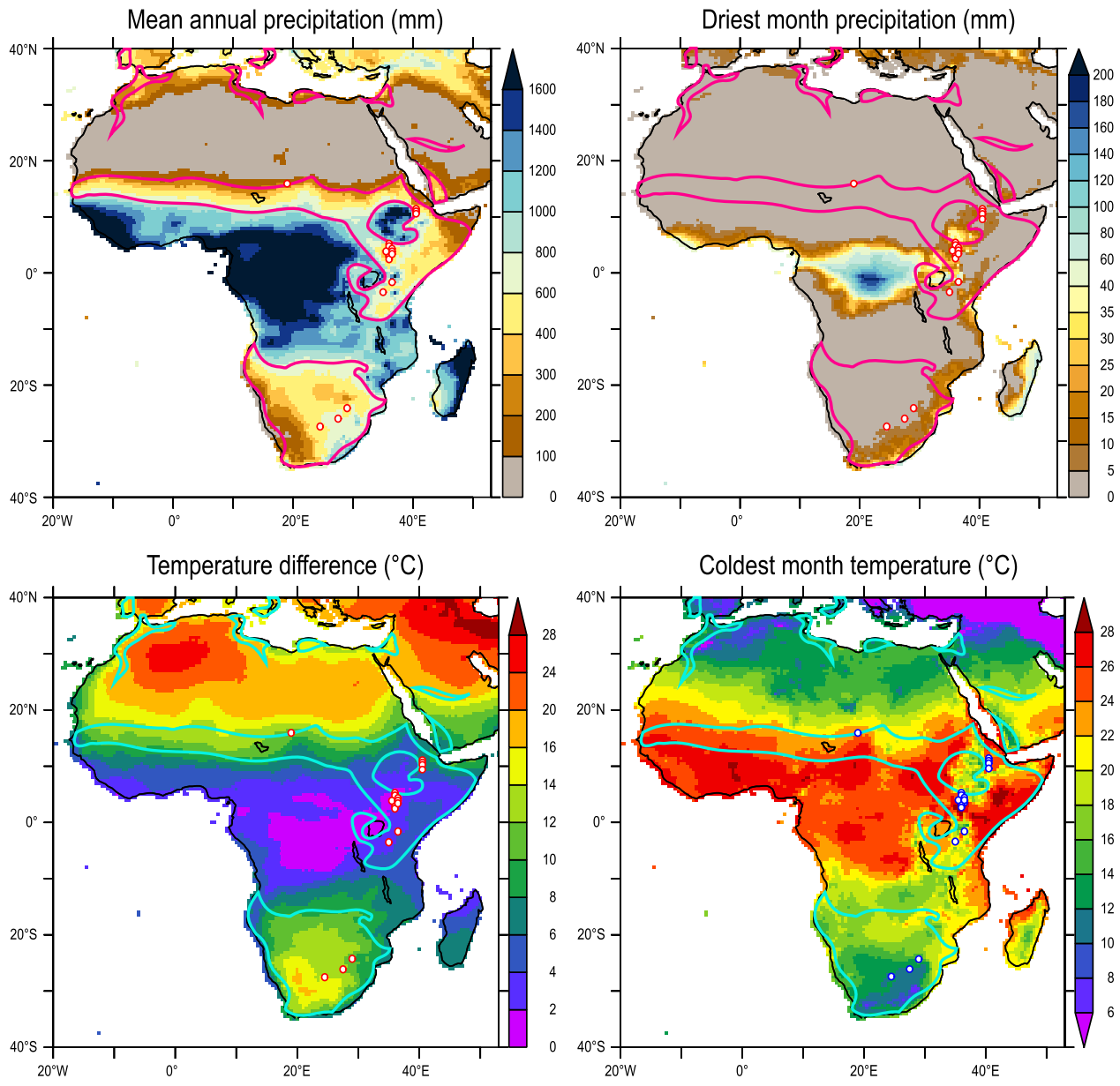

Fig. 3. Mean annual precipitation (MAP), driest month precipitation (DMP), temperature difference between the coldest and warmest months (DT), and coldest month temperature for the Pliocene (CMT). Areas suitable for hominins from Figure 2 are outlined. MAP and DT are the variables composing the "best" parameter setting selected after model calibration.

et al., 2019). However not all early hominids are associated with savannahs, *Orrorrin* lived in an open deciduous forest, punctuated by very wet areas (Bamford et al., 2013; Senut, 2020).

By the late Pliocene, *Australopithecus* occupied open landscape environments. Pliocene hominin localities of the Lower Awash Valley and the Turkana Basin had mammal communities corresponding to a climate for which precipitation was low (inferior to 800–1000 mm/yr) and temperature seasonality was pronounced (Robinson et al., 2017). Our model suggests that these populations occupied regions characterized by a semi-arid climate (dry and seasonal with moderate thermal amplitude) and environments that would have been more or less wooded depending on surface and sub-surface water availability. Blumenthal et al. (2017) postulate that variable climatic conditions in the Turkana Basin, within the range of present-day environments, were already present at 4.2 Ma, suggesting that the region's hominins were already occupying (semi-) arid areas with soil temperatures of approximately 30–35 °C (Passey et al., 2010). Sponheimer (2013) also states that the australopithecine masticatory apparatus was adapted to abrasive food already by 4 Ma, implying that they could rely on (although perhaps only seasonally) xerophytic tubers which are found in arid environments and can contain up to 70% water.

A re-examination of Turkana *Au. anamensis* has shown that C_4 biomass composed up to 30% of their diet, suggesting increased foraging in open landscapes already by 4 Ma (Quinn, 2019). An increased proportion of C_4 foods in the hominin diet occurs at 3.8 Ma (Uno et al., 2016), and *Au. bahrelghazali* was also dependent of C_4-derived resources (Lee-Thorp et al., 2012). At Hadar, *Au. afarensis* was a mixed C_3/C_4 feeder and coped with ecological changes via "… a highly varied intake of C_4 foods" (Wynn et al., 2016). Recent dental analyses of *Au. africanus* also reveal that this species faced seasonal dietary stress (Joannes-Boyau et al., 2019). Finally, our results show that the climate envelope of mid-to-late Pliocene hominins largely overlaps with semi-arid climates, but

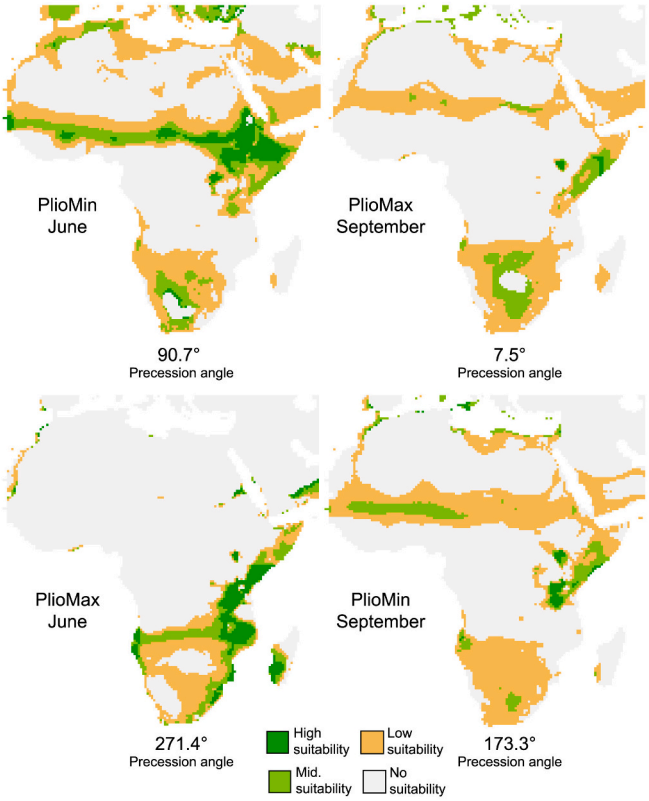

Fig. 4. Projections of the final model computed with the Pliocene mean configuration onto four orbital precession configurations (see Methods). PlioMax June with a precesion angle of 271° is the most distant configuration from Pliocene 'mean' climate (i.e. 100.04°), whereas PlioMin June is the closest (90.74°).

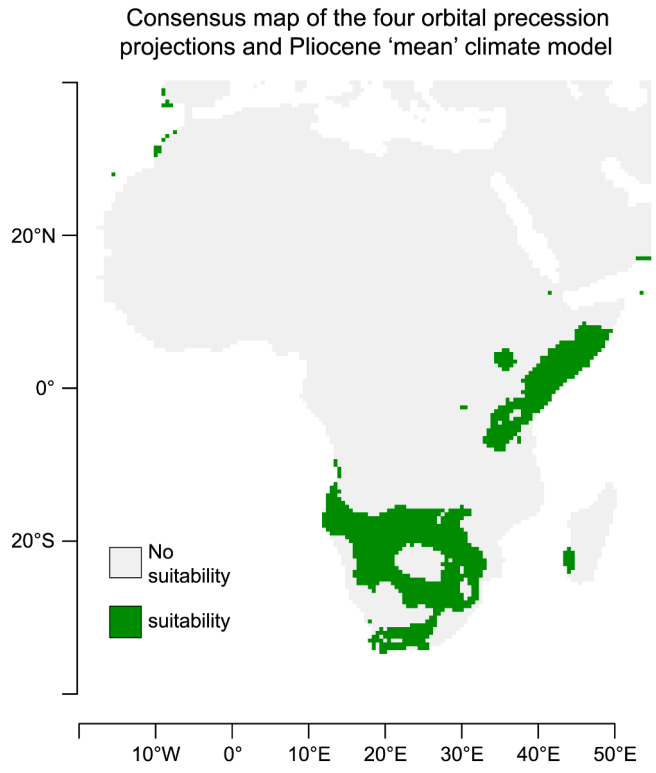

Fig. 5. Refuge areas. Consensus map based on the final climatic envelope's suitable areas estimated with Pliocene 'mean' climate (Fig. 2), as well as with the four orbital precession configurations (Fig. 4).

also includes more temperate climates. This agrees with Behrensmeyer and Reed (2013) who consider that *Australopithecus* could survive "considerable seasonal temperature" variations, thus suggesting that they possessed enhanced thermoregulatory capacities (Lieberman, 2015). This is a step toward the genus *Homo*, which appears to have been adapted to even more arid climates (DiMaggio et al., 2015; Robinson et al., 2017).

4.2. Hypotheses on the paleobiogeography of Australopithecus

Dispersal events during the Pliocene are thought to have strongly influenced the paleobiogeography of *Australopithecus* (Foley, 2013). Our results support this hypothesis by indicating that australopithecines in Chad, eastern Africa and South Africa faced similar climatic conditions. However, the dispersal of early hominins between eastern Africa and southern Africa appears to have been possible only during periods of extreme summer insolation (PlioMax June), when the Lake Malawi basin would have been dry enough to create continuous semi-arid environments (Fig. 4 and Suppl. Figure 5). To the contrary, *Au. bahrelghazali*, *Au. afarensis,* and *K. platyops* could have dispersed between the Turkana Basin, Laetoli and the SKT region, the Awash Valley and central Sahel—with the Turkana basin and the SKT region remaining suitable during periods of extreme insolation forcing. Isolation of some regions (e.g., the Turkana Basin and SKT regions serving as refugia), induced by climate and vegetation changes driven by orbital forcing, would have isolated animal populations (including hominids) and reduced gene flow, thus fostering allopatric speciation by vicariance. This would explain the highest levels of species diversity in eastern Africa: distinct species could develop during periods when the two regions were not connected, and later disperse during periods when they were environmentally linked. Comparing the habitat suitability map to the vegetation model (Figs. 1 and 2), it is evident that areas of suitability correspond primarily to those where the simulated biome is tropical xerophytic shrubland (represented in pink in Fig. 1), although the two maps are not strictly superimposable. This environment is typically present along woodland margins (fringe environments), corresponding to the hypothesis that *Australopithecus* was an edge (or ecotonal) adapted genus (Sussman and Hart, 2015), as suggested for early Pleistocene *Paranthropus robustus* (Caley et al., 2018).

According to our results, the coastal regions of southern Somalia and eastern Kenya would have been suitable for all precession-driven insolation states (Fig. 5). This region is included in the extent of the coastal mosaic forest proposed by Kingdon (2003) and Joordens et al. (2019) (the coastal ape hypothesis). However, our vegetation model does not reproduce forest in this area, but rather tropical xerophytic shrubland (this biome does contain the tropical raingreen tree plant functional type); our model also supports the hypothesis that *Australopithecus* did not live in forest contexts, but rather in semi-arid zones. Small-scale patches of gallery forest could have been favoured by local conditions (e.g. lake, river) in this area, without being visible in the model, since the coastal forest at present only measures a few tens of kilometres of width at its maximum extent. The fact that occurrence points of Pliocene *Australopithecus* are located in semi-arid areas, which were already semi-arid areas during the Pliocene, does not mean that these species were restricted solely to these areas, since it remains possible that fossils have not been observed elsewhere. Our model, which effectively indicates areas where remains have been recovered, does predict that this region of southern Kenya and northern Tanzania had some tropical trees, and was climatically favourable for *Australopithecus* during the Pliocene even across climate changes linked to orbital precession variability.

5. Conclusions

During the mid-to-late Pliocene, different hominin species are identified in Africa at localities that are geographically separated (central Sahel, eastern Africa and southern Africa). When using a climatic envelope model, the estimated areas suitable for mid-to-late Pliocene hominins cover most of eastern Africa, the Sahelian corridor from the Atlantic coast to the Red Sea, large portions of southern Africa, and a restricted portion of the African northwestern Mediterranean coast. The climatic envelope associated with these areas is predominantly characterized by strongly seasonal precipitation and annual thermal amplitude up to 15 °C, in accordance with the two variables selected by the kuenm R package to create the final model (i.e., mean annual precipitation and thermal amplitude between coldest and warmest month). The estimated envelope is geographically continuous between eastern Africa and the Lake Chad region, while a similar pattern is not observed between eastern Africa and southern Africa, suggesting that this environmental barrier was crossed during periods of extreme summer insolation maxima or that hominins had a broader climatic envelope than the one estimated with our occurrence data. The Turkana Basin, the region covering southern Somalia, eastern Kenya and northern Tanzania (including Laetoli and coastal regions), and a vast portion of southern Africa remain suitable during periods of orbital variability, contrary to the Sahelian corridor and the Awash valley. Those refugia are located in eastern and southern Africa and are only connected during certain orbital configurations, potentially explaining the diversity of hominin species observed in eastern Africa at that time.

Further studies could improve our results, notably, due to the scarce nature of presently available data, but this is certainly a long-term perspective. For the immediate future, the increased capability of climate models to simulate Pliocene conditions via PLIOMIP2 (Haywood et al., 2020; Tan et al., 2020; Zhang et al., 2021) warrants pursuing.

Declaration of Competing Interest

The authors declare that they have no known competing financial interests or personal relationships that could have appeared to influence the work reported in this paper.

Acknowledgments

This research was conducted within the framework of the ANR projet HADoC (ANR-17-CE31-0010). The authors were granted access to the HPC resources of TGCC under the allocation 2019-A0050102212 made possible by GENCI. We thank both reviewers for their suggestions and improvements.

Appendix A. Supplementary data

Supplementary data to this article can be found online at https://doi.org/10.1016/j.gloplacha.2022.103756.

References

Alemseged, Z., Spoor, F., Kimbel, W.H., Bobe, R., Geraads, D., Reed, D., Wynn, J.G., 2006. A juvenile early hominin skeleton from Dikika, Ethiopia. Nature 443 (7109), 296–301. https://doi.org/10.1038/nature05047.

Anderson, R.P., Raza, A., 2010. The effect of the extent of the study region on GIS models of species geographic distributions and estimates of niche evolution: preliminary tests with montane rodents (genus *Nephelomys*) in Venezuela. J. Biogeogr. 37 (7), 1378–1393. https://doi.org/10.1111/j.1365-2699.2010.02290.x.

Araújo, M.B., Peterson, A.T., 2012. Uses and misuses of bioclimatic envelope modeling. Ecology 93, 1527–1539. https://doi.org/10.1890/11-1930.1.

Bamford, M.K., Senut, B., Pickford, M., 2013. Fossil leaves from Lukeino, a 6-million-year-old Formation in the Baringo Basin, Kenya. Geobios 46 (4), 253–272. https://doi.org/10.1016/j.geobios.2013.02.001.

Barboni, D., Ashley, G.M., Bourel, B., Arráiz, H., Mazur, J.-C., 2019. Springs, palm groves, and the record of early hominins in Africa. Rev. Palaeobot. Palynol. 266, 23–41. https://doi.org/10.1016/j.revpalbo.2019.03.004.

Barve, N., Barve, V., Jiménez-Valverde, A., Lira-Noriega, A., Maher, S.P., Peterson, A.T., Villalobos, F., 2011. The crucial role of the accessible area in ecological niche modeling and species distribution modeling. Ecol. Modell. 222 (11), 1810–1819.

Behrensmeyer, A.K., Reed, K.E., 2013. Reconstructing the habitats of *Australopithecus*: paleoenvironments, site taphonomy, and faunas. In: Reed, K.E., Fleagle, J.G., Leakey, R.E. (Eds.), The Paleobiology of *Australopithecus*. Springer, Dordrecht, pp. 41–60. https://doi.org/10.1007/978-94-007-5919-0_4.

Blondel, C., Merceron, G., Andossa, L., Taisso, M.H., Vignaud, P., Brunet, M., 2010. Dental mesowear analysis of the late Miocene Bovidae from Toros-Menalla (Chad) and early hominid habitats in Central Africa. Palaeogeogr. Palaeoclimatol. Palaeoecol. 292, 184–191. https://doi.org/10.1016/j.palaeo.2010.03.042.

Blumenthal, S.A., Levin, N.E., Brown, F.H., Brugal, J.P., Chritz, K.L., Harris, J.M., Jehle, G.E., Cerling, T.E., 2017. Aridity and hominin environments. Proc. Natl. Acad. Sci. U. S. A. 114 (28), 7331–7336. https://doi.org/10.1073/pnas.1700597114.

Boës, X., Prat, S., Arrighi, V., Feibel, C., Haileab, B., Lewis, J., Harmand, S., 2019. Lake-level changes and hominin occupations in the arid Turkana basin during volcanic closure of the Omo River outflows to the Indian Ocean. Quat. Res. 91 (2), 892–909. https://doi.org/10.1017/qua.2018.118.

Bonnefille, R., Potts, R., Chalie, F., Jolly, D., Peyron, O., 2004. High-resolution vegetation and climate change associated with Pliocene *Australopithecus afarensis*. Proc. Natl. Acad. Sci. U. S. A. 101, 12125–12129. https://doi.org/10.1073/pnas.0401709101.

Brown, F.H., McDougall, I., Gathogo, P.N., 2013. Age Ranges of *Australopithecus* species, Kenya, Ethiopia, and Tanzania. In: Reed, K.E., Fleagle, J.G., Leakey, R.E. (Eds.), The Paleobiology of *Australopithecus*. Springer, Dordrecht, pp. 7–20. https://doi.org/10.1007/978-94-007-5919-0_2.

Brunet, M., Beauvilain, A., Coppens, Y., Heintz, E., Moutaye, A.H.E., Pilbeam, D., 1995. The first australopithecine 2,500 kilometres west of the Rift Valley (Chad). Nature 378, 273–275. https://doi.org/10.1038/378273a0.

Brunet, M., Beauvilain, A., Coppens, Y., Heintz, E., Moutaye, A.H.E., Pilbeam, D., 1996. *Australopithecus bahrelghazali*, une nouvelle espèce d'Hominidé ancien de la région de Koro Toro (Tchad). C. R. Acad. Sci. Paris 322, 907–913.

Bruxelles, L., Stratford, D.J., Maire, R., Pickering, T.R., Heaton, J.L., Beaudet, A., Kuman, K., Crompton, R., Carlson, K.J., Jashashvili, T., McClymont, J., Leader, G.M., Clarke, R.J., 2019. A multiscale stratigraphic investigation of the context of StW 573 'Little Foot'and Member 2, Sterkfontein Caves, South Africa. J. Hum. Evol. 133, 78–98. https://doi.org/10.1016/j.jhevol.2019.05.008.

Caley, T., Extier, T., Collins, J.A., Schefuß, E., Dupont, L., Malaizé, B., Rossignol, L., Souron, A., McClymont, E.L., Jimenez-Espejo, F.J., García-Comas, C., Eynaud, F., Martinez, P., Roche, D.M., Jorry, S.J., Charlier, K., Wary, M., Gourves, P.-Y., Billy, I., Giraudeau, J., 2018. A two-million-year-long hydroclimatic context for hominin evolution in southeastern Africa. Nature 560 (7716), 76–79. https://doi.org/10.1038/s41586-018-0309-6.

Cerling, T.E., Wynn, J.G., Andanje, S.A., Bird, M.I., Korir, D.K., Levin, N.E., Mace, W., Macharia, A.N., Quade, J., Remien, C.H., 2011. Woody cover and hominin environments in the past 6 million years. Nature 476 (7358), 51–56. https://doi.org/10.1038/nature10306.

Clarke, R.J., Kuman, K., 2019. The skull of StW 573, a 3.67 Ma *Australopithecus prometheus* skeleton from Sterkfontein Caves, South Africa. J. Hum. Evol. 134, 102634 https://doi.org/10.1016/j.jhevol.2019.06.005.

Cobos, M.E., Peterson, A.T., Barve, N., Osorio-Olvera, L., 2019. Kuenm: an R package for detailed development of ecological niche models using Maxent. PeerJ 7, e6281. https://doi.org/10.7717/peerj.6281.

Contoux, C., Ramstein, G., Jost, A., 2012. Modelling the mid-Pliocene warm period climate with the IPSL coupled model and its atmospheric component LMDZ5A. Geosci. Model Dev. 5, 903–917. https://doi.org/10.5194/gmd-5-903-2012.

Contoux, C., Dumas, C., Ramstein, G., Jost, A., Dolan, A.M., 2015. Modelling Greenland ice sheet inception and sustainability during the late Pliocene. Earth Planet. Sci. Lett. 424, 295–305. https://doi.org/10.1016/j.epsl.2015.05.018.

Coulthard, T.J., Ramirez, J.A., Barton, N., Rogerson, M., Brücher, T., 2013. Were rivers flowing across the Sahara during the last interglacial? Implications for human migration through Africa. PLoS One 8 (9), e74834. https://doi.org/10.1371/journal.pone.0074834.

Curran, S.C., Haile-Selassie, Y., 2016. Paleoecological reconstruction of hominin-bearing middle Pliocene localities at Woranso-Mille, Ethiopia. J. Hum. Evol. 96, 97–112. https://doi.org/10.1016/j.jhevol.2016.04.002.

Dart, R.A., 1925. *Australopithecus africanus*: the man-ape of South Africa. Nature 115, 195–199.

De La Vega, E., Chalk, T.B., Wilson, P.A., Bysani, R.P., Foster, G.L., 2020. Atmospheric CO 2 during the mid-piacenzian warm period and the M2 glaciation. Sci. Rep. 10 (1), 1–8. https://doi.org/10.1038/s41598-020-67154-8.

De Schepper, S., Gibbard, P.L., Salzmann, U., Ehlers, J., 2014. A global synthesis of the marine and terrestrial evidence for glaciation during the Pliocene Epoch. Earth-Sci. Rev. 135, 83–102. https://doi.org/10.1016/j.earscirev.2014.04.003.

Deino, A.L., Scott, G.R., Saylor, B., Alene, M., Angelini, J.D., Haile-Selassie, Y., 2010. 40Ar/39Ar dating, paleomagnetism, and tephrochemistry of Pliocene strata of the hominid-bearing Woranso-Mille area, west-Central Afar Rift, Ethiopia. J. Hum. Evol. 58 (2), 111–126. https://doi.org/10.1016/j.jhevol.2009.11.001.

DiMaggio, E.N., Campisano, C.J., Rowan, J., Dupont-Nivet, G., Deino, A.L., Bibi, F., Lewis, M.E., Souron, A., Garello, D., Werdelin, L., Reed, K.E., Arrowsmith, J.R., 2015. Late Pliocene fossiliferous sedimentary record and the environmental context of early *Homo* from Afar, Ethiopia. Science 347 (6228), 1355–1359. https://doi.org/10.1126/science.aaa1415.

Dowsett, H., Dolan, A., Rowley, D., Moucha, R., Forte, A.M., Mitrovica, J.X., Haywood, A., 2016. The PRISM4 (mid-Piacenzian) paleoenvironmental

reconstruction. Clim. Past 12 (7), 1519–1538. https://doi.org/10.5194/cp-12-1519-2016.

Dufresne, J.-L., Foujols, M.-A., Denvil, S., Caubel, A., Marti, O., Aumont, O., Balkanski, Y., Bekki, S., Bellenger, H., Benshila, R., Bony, S., Bopp, L., Braconnot, P., Brockmann, P., Cadule, P., Cheruy, F., Codron, F., Cozic, A., Cugnet, D., de Noblet, N., Duvel, J.-P., Ethé, C., Fairhead, L., Fichefet, T., Flavoni, S., Friedlingstein, P., Grandpeix, J.-Y., Guez, L., Guilyardi, E., Hauglustaine, D., Hourdin, F., Idelkadi, A., Ghattas, J., Joussaume, S., Kageyama, M., Krinner, G., Labetoulle, S., Lahellec, A., Lefebvre, M.-P., Lefevre, F., Levy, C., Li, Z.X., Lloyd, J., Lott, F., Madec, G., Mancip, M., Marchand, M., Masson, S., Meurdesoif, Y., Mignot, J., Musat, I., Parouty, S., Polcher, J., Rio, C., Schulz, M., Swingedouw, D., Szopa, S., Talandier, C., Terray, P., Viovy, N., Vuichard, N., 2013. Climate change projections using the IPSL-CM5 Earth System Model: from CMIP3 to CMIP5. Clim. Dyn. 40 (9), 2123–2165. https://doi.org/10.1007/s00382-012-1636-1.

Elith, J., Graham, C.H., Anderson, R.P., Dudík, M., Ferrier, S., Guisan, A., Hijmans, R.J., Huettmann, F., Leathwick, J.R., Lehmann, A., Li, J., Lohmann, L.G., Loiselle, B.A., Manion, G., Moritz, C., Nakamura, M., Nakazawa, Y., Overton, J., Peterson, A.T., Phillips, S.J., Richardson, K., Scachetti-Pereira, R., Schapire, R.E., Zimmermann, N. E., 2006. Novel methods improve prediction of species' distributions from occurrence data. Ecography 29 (2), 129–151. https://doi.org/10.1111/j.2006.0906-7590.04596.x.

Feibel, C.S., 2011. A Geological history of the Turkana Basin. Evol. Anthropol. 20, 206–216. https://doi.org/10.1002/evan.20331.

Fleagle, J.G., Rasmussen, D.T., Yirga, S., Bown, T.M., Grine, F.E., 1991. New hominid fossils from Fejej, Southern Ethiopia. J. Hum. Evol. 21, 145–152. https://doi.org/10.1016/0047-2484(91)90005-G.

Foley, R.A., 2013. Comparative Evolutionary Models and the "Australopith Radiations". In: Reed, K.E., Fleagle, J.G., Leakey, R.E. (Eds.), The Paleobiology of *Australopithecus*. Springer, Dordrecht, pp. 163–174. https://doi.org/10.1007/978-94-007-5919-0_10.

Good, S.P., Caylor, K.K., 2011. Climatological determinants of woody cover in Africa. Proc. Natl. Acad. Sci. U. S. A. 108 (12), 4902–4907. https://doi.org/10.1073/pnas.1013100108.

Guisan, A., Thuiller, W., Zimmermann, N.E., 2017. Habitat Suitability and Distribution Models: With Applications in R. Cambridge University Press, Cambridge, UK.

Haile-Selassie, Y., Saylor, B.Z., Deino, A., Levin, N.E., Alene, M., Latimer, B.M., 2012. A new hominin foot from Ethiopia shows multiple Pliocene bipedal adaptations. Nature 483 (7391), 565–569. https://doi.org/10.1038/nature10922.

Haile-Selassie, Y., Gibert, L., Melillo, S.M., Ryan, T.M., Alene, M., Deino, A., Levin, N.E., Scott, G., Saylor, B.Z., 2015. New species from Ethiopia further expands Middle Pliocene hominin diversity. Nature 521 (7553), 483–488. https://doi.org/10.1038/nature14448.

Haile-Selassie, Y., Melillo, S.M., Vazzana, A., Benazzi, S., Ryan, T.M., 2019. A 3.8-million-year-old hominin cranium from Woranso-Mille, Ethiopia. Nature 573, 214–219. https://doi.org/10.1038/s41586-019-1513-8.

Harmand, S., Lewis, J.E., Feibel, C.S., Lepre, C.J., Prat, S., Lenoble, A., Harmand, S., Lewis, J.E., Feibel, C.S., Lepre, C.J., Prat, S., Lenoble, A., Boës, X., Quinn, R.L., Brenet, M., Arroyo, A., Taylor, N., Clément, S., Daver, G., Brugal, J.-P., Leakey, L., Mortlock, R.A., Wright, J.D., Lokorodi, S., Kirwa, C., Kent, D.V., Roche, H., 2015. 3.3-million-year-old stone tools from Lomekwi 3, West Turkana, Kenya. Nature 521 (7552), 310–315. https://doi.org/10.1038/nature14464.

Harrison, S.P., Prentice, C.I., 2003. Climate and CO2 controls on global vegetation distribution at the last glacial maximum: analysis based on palaeovegetation data, biome modelling and palaeoclimate simulations. Glob. Change Biol. 9 (7), 983–1004.

Haywood, A.M., Dowsett, H.J., Otto-Bliesner, B., Chandler, M.A., Dolan, A.M., Hill, D.J., Robinson, M.M., Rosenbloom, N., Salzmann, U., Sohl, L.E., 2010. Pliocene model intercomparison project (PlioMIP): experimental design and boundary conditions (experiment 1). Geosci. Model Dev. 3 (1), 227–242. https://doi.org/10.5194/gmd-3-227-2010.

Haywood, A.M., Dowsett, H.J., Robinson, M.M., Stoll, D.K., Dolan, A.M., Lunt, D.J., Otto-Bliesner, B., Chandler, M.A., 2011. Pliocene Model Intercomparison Project (PlioMIP): experimental design and boundary conditions (Experiment 2). Geosci. Model Dev. 4, 571–577. https://doi.org/10.5194/gmd-4-571-2011.

Haywood, A.M., Tindall, J.C., Dowsett, H.J., Dolan, A.M., Foley, K.M., Hunter, S.J., Hill, D.J., Chan, W.-L., Abe-Ouchi, A., Stepanek, C., Lohmann, G., Chandan, D., Peltier, W.R., Tan, N., Contoux, C., Ramstein, G., Li, X., Zhang, Z., Guo, C., Nisancioglu, K.H., Zhang, Q., Li, Q., Kamae, Y., Chandler, M.A., Sohl, L.E., Otto-Bliesner, B.L., Feng, R., Brady, E.C., von der Heydt, A.S., Baatsen, M.L.J., Lunt, D.J., 2020. The Pliocene Model Intercomparison Project phase 2: large-scale climate features and climate sensitivity. Clim. Past 16, 2095–2123. https://doi.org/10.5194/cp-16-2095-2020.

Hély, C., Braconnot, P., Watrin, J., Zheng, W., 2009. Climate and vegetation: simulating the African humid period. C. R. Geoscience 341, 671–688. https://doi.org/10.1016/j.crte.2009.07.002.

Hernandez, P.A., Graham, C.H., Master, L.L., Albert, D.L., 2006. The effect of sample size and species characteristics on performance of different species distribution modeling methods. Ecography 29, 773–785. https://doi.org/10.1111/j.0906-7590.2006.04700.x.

Herries, A.I., Pickering, R., Adams, J.W., Curnoe, D., Warr, G., Latham, A.G., Shaw, J., 2013. A multi-disciplinary perspective on the age of *Australopithecus* in southern Africa. In: Reed, K.E., Fleagle, J.G., Leakey, R.E. (Eds.), The Paleobiology of *Australopithecus*. Springer, Dordrecht, pp. 21–40. https://doi.org/10.1007/978-94-007-5919-0_3.

Joannes-Boyau, R., Adams, J.W., Austin, C., Arora, M., Moffat, I., Herries, A.I.R., Tonge, M.P., Benazzi, S., Evans, A.R., Kullmer, O., Wroe, S., Dosseto, A., Fiorenza, L., 2019. Elemental signatures of *Australopithecus africanus* teeth reveal seasonal dietary stress. Nature 572 (7767), 112–115. https://doi.org/10.1038/s41586-019-1370-5.

Joordens, J.C.A., Feibel, C.S., Vonhof, H.B., Schulp, A.S., Kroon, D., 2019. Relevance of the eastern African coastal forest for early hominin biogeography. J. Hum. Evol. 131, 176–202. https://doi.org/10.1016/j.jhevol.2019.03.012.

Kageyama, M., Braconnot, P., Bopp, L., Caubel, A., Foujols, M.-A., Guilyardi, E., Khodri, M., Lloyd, J., Lombard, F., Mariotti, V., Marti, O., Roy, T., Woillez, M.-N., 2013. Mid-Holocene and last Glacial Maximum climate simulations with the IPSL model—part I: comparing IPSL_CM5A to IPSL_CM4. Clim. Dyn. 40 (9–10), 2447–2468. https://doi.org/10.1007/s00382-012-1488-8.

Kaplan, J.O., Bigelow, N.H., Prentice, I.C., Harrison, S.P., Bartlein, P.J., Christensen, T. R., Cramer, W., Matveyeva, N.V., McGuire, A.D., Murray, D.F., Razzhivin, V.Y., Smith, B., Walker, D.A., Anderson, P.M., Andreev, A.A., Brubaker, L.B., Edwards, M. E., Lozhkin, A.V., 2003. Climate change and Arctic ecosystems: 2. Modeling, paleodata-model comparisons, and future projections. J. Geophys. Res. Atmos. 108 (D19), 8171. https://doi.org/10.1029/2002JD002559.

Kappelman, J., Swisher III, C.C., Fleagle, J.G., Yirga, S., Bown, T.M., Feseha, M., 1996. Age of *Australopithecus afarensis* from Fejej, Ethiopia. J. Hum. Evol. 30 (2), 139–146.

Kingdon, J., 2003. Lowly Origin: Where, When, and Why Our Ancestors First Stood Up. Princeton University Press, Princeton. https://doi.org/10.1073/pnas.1807912115.

Krinner, G., Flanner, M.G., 2018. Striking stationarity of large-scale climate model bias patterns under strong climate change. Proc. Natl. Acad. Sci. U. S. A. 115 (38), 9462–9466.

Kröpelin, S., Verschuren, D., Lézine, A.M., Eggermont, H., Cocquyt, C., Francus, P., Cazet, J.-P., Fagot, M., Rumes, B., Russell, J.M., Darius, F., Conley, D.J., Schuster, M., von Suchodoletz, H., Engstrom, D.R., 2008. Climate-driven ecosystem succession in the Sahara: the past 6000 years. Science 320 (5877), 765–768. https://doi.org/10.1126/science.1154913.

Kullmer, O., Sandrock, O., Viola, T.B., Hujer, W., Said, H., Seidler, H., 2008. Suids, elephantoids, paleochronology, and paleoecology of the Pliocene hominid site Galili, Somali Region, Ethiopia. Palaios 23 (7), 452–464. https://doi.org/10.2110/palo.2007.p07-028r.

Le Fur, S., Fara, E., Mackaye, H.T., Vignaud, P., Brunet, M., 2009. The mammal assemblage of the hominid site TM266 (late Miocene, Chad Basin): ecological structure and paleoenvironmental implications. Naturwissenschaften 96, 565–574. https://doi.org/10.1007/s00114-008-0504-7.

Leakey, M.G., Walker, A.C., 2003. The Lothagam hominids. In: Leakey, M.G., Harris, J.M. (Eds.), Lothagam. Columbia University Press, New York, pp. 249–258. https://doi.org/10.7312/leak11870.

Leakey, M.G., Feibel, C.S., McDougall, I., Ward, C., Walker, A., 1998. New specimens and confirmation of an early age for *Australopithecus anamensis*. Nature 393, 62–66. https://doi.org/10.1038/29972.

Leakey, M.G., Spoor, F., Brown, F.H., Gathogo, P.N., Kiarie, C., Leakey, L.N., McDougall, I., 2001. New hominin genus from eastern Africa shows diverse middle Pliocene lineages. Nature 410 (6827), 433–440. https://doi.org/10.1038/35068500.

Lebatard, A.-E., Bourlès, D.L., Duringer, P., Jolivet, M., Braucher, R., Carcaillet, J., Schuster, M., Arnaud, N., Monié, P., Lihoreau, F., Likius, A., Mackaye, H.T., Vignaud, P., Brunet, M., 2008. Cosmogenic nuclide dating of *Sahelanthropus tchadensis* and *Australopithecus bahrelghazali*: Mio-Pliocene hominids from Chad. Proc. Natl. Acad. Sci. U. S. A. 105 (9), 3226–3231. https://doi.org/10.1073/pnas.0708015105.

Lee-Thorp, J., Likius, A., Mackaye, H.T., Vignaud, P., Sponheimer, M., Brunet, M., 2012. Isotopic evidence for an early shift to C4 resources by Pliocene hominins in Chad. Proc. Natl. Acad. Sci. U. S. A. 109 (50), 20369–20372. https://doi.org/10.1073/pnas.1204209109.

Levin, N.E., Simpson, S.W., Quade, J., Cerling, T.E., Frost, S.R., 2008. Herbivore enamel carbon isotopic composition and the environmental context of *Ardipithecus* at Gona, Ethiopia. In: Quade, J., Wynn, J.G. (Eds.), The Geology of Early Humans in the Horn of Africa. Geological Society of America, pp. 215–234. https://doi.org/10.1130/2008.2446(10).

Lieberman, D.E., 2015. Human locomotion and heat loss: an evolutionary perspective. Compr. Physiol. 5, 99–117. https://doi.org/10.1002/cphy.c140011.

Lisiecki, L.E., Raymo, M.E., 2005. A Pliocene-Pleistocene stack of 57 globally distributed benthic $\delta^{18}O$ records. Paleoceanography 20 (1), PA1003. https://doi.org/10.1029/2004PA001071.

Marston, C.G., Wilkinson, D.M., Reynolds, S.C., Louys, J., O'Regan, H.J., 2019. Water availability is a principal driver of large-scale land cover spatial heterogeneity in sub-Saharan savannahs. Landsc. Ecol. 34 (1), 131–145. https://doi.org/10.1007/s10980-018-0750-9.

Mbua, E., Kusaka, S., Kunimatsu, Y., Geraads, D., Sawada, Y., Brown, F.H., Sakai, T., Boisserie, J.-R., Saneyoshi, M., Omuombo, C., Muteti, S., Hirata, T., Hayashida, A., Iwano, H., Danhara, T., Bobe, R., Jicha, B., Nakatsukasa, M., 2016. Kantis: a new *Australopithecus* site on the shoulders of the Rift Valley near Nairobi, Kenya. J. Hum. Evol. 94, 28–44. https://doi.org/10.1016/j.jhevol.2016.01.006.

Merow, C., Smith, M.J., Silander, J.A., 2013. A practical guide to MaxEnt for modeling species' distributions: what it does, and why inputs and settings matter. Ecography 36, 1058–1069. https://doi.org/10.1111/j.1600-0587.2013.07872.x.

New, M., Lister, D., Hulme, M., Makin, I., 2002. A high-resolution data set of surface climate over global land areas. Clim. Res. 21, 1–25. https://doi.org/10.3354/cr021001.

Novello, A., Barboni, D., Sylvestre, F., Lebatard, A.-E., Paillès, C., Bourlès, D.L., Likius, A., Mackaye, H.T., Vignaud, P., Brunet, M., 2017. Phytoliths indicate significant arboreal cover at *Sahelanthropus* type locality TM266 in northern Chad and a decrease in later sites. J. Hum. Evol. 106, 66–83. https://doi.org/10.1016/j.jhevol.2017.01.009.

Owens, H.L., Campbell, L.P., Dornak, L.L., Saupe, E.E., Barve, N., Soberón, J., Ingenloff, K., Lira-Noriega, A., Hensz, C.M., Myers, C.E., Peterson, A.T., 2013. Constraints on interpretation of ecological niche models by limited environmental ranges on calibration areas. Ecol. Model. 263, 10–18. https://doi.org/10.1016/j.ecolmodel.2013.04.011.

Paillard, D., Labeyrie, L.D., Yiou, P., 1996. AnalySeries 1.0: a Macintosh software for the analysis of geophysical time-series. Eos 77, 379.

Passey, B.H., Levin, N.E., Cerling, T.E., Brown, F.H., Eiler, J.M., 2010. High-temperature environments of human evolution in East Africa based on bond ordering in paleosol carbonates. Proc. Natl. Acad. Sci. U. S. A. 107, 11245–11249. https://doi.org/10.1073/pnas.1001824107.

Pearson, R.G., Raxworthy, C.J., Nakamura, M., Peterson, A.T., 2006. Predicting species distributions from small numbers of occurrence records: a test case using cryptic geckos in Madagascar. J. Biogeogr. 34, 102–117. https://doi.org/10.1111/j.1365-2699.2006.01594.x.

Peel, M.C., Finlayson, B.L., McMahon, T.A., 2007. Updated world map of the Köppen-Geiger climate classification. Hydrol. Earth Syst. Sci. 11 (5), 1633–1644. https://doi.org/10.5194/hess-11-1633-2007.

Peterson, A.T., Papeş, M., Eaton, M., 2007. Transferability and model evaluation in ecological niche modeling: a comparison of GARP and Maxent. Ecography 30 (4), 550–560. https://doi.org/10.1111/j.0906-7590.2007.05102.x.

Peterson, A.T., Papeş, M., Soberón, J., 2008. Rethinking receiver operating characteristic analysis applications in ecological niche modeling. Ecol. Model. 213, 63–72. https://doi.org/10.1016/j.ecolmodel.2007.11.008.

Peterson, A.T., Soberón, J., Pearson, R.G., Anderson, R.P., Martínez-Meyer, E., Nakamura, M., Araújo, M.B., 2011. Ecological Niches and Geographic Distributions (MPB-49). Princeton University Press, Princeton. https://doi.org/10.1515/9781400840670.

Peterson, A.T., Cobos, M.E., Jiménez-García, D., 2018. Major challenges for correlational ecological niche model projections to future climate conditions. Ann. N. Y. Acad. Sci. 1429 (1), 66–77. https://doi.org/10.1111/nyas.13873.

Phillips, S.J., Dudík, M., 2008. Modeling of species distributions with Maxent: new extensions and a comprehensive evaluation. Ecography 31, 161–175. https://doi.org/10.1111/j.0906-7590.2008.5203.x.

Phillips, S.J., Anderson, R.P., Schapire, R.E., 2006. Maximum entropy modeling of species geographic distributions. Ecol. Model. 190, 231–259. https://doi.org/10.1016/j.ecolmodel.2005.03.026.

Phillips, S.J., Anderson, R.P., Dudík, M., Schapire, R.E., Blair, M.E., 2017. Opening the black box: an open-source release of Maxent. Ecography 40, 887–893. https://doi.org/10.1111/ecog.03049.

Pound, M.J., Tindall, J., Pickering, S.J., Haywood, A.M., Dowsett, H.J., Salzmann, U., 2014. Late Pliocene lakes and soils: a global data set for the analysis of climate feedbacks in a warmer world. Clim. Past 10 (1), 167–180. https://doi.org/10.5194/cp-10-167-2014.

Quade, J., Dente, E., Armon, M., Dor, Y.B., Morin, E., Adam, O., Enzel, Y., 2018. Megalakes in the Sahara? A review. Quat. Res. 90 (2), 253–275. https://doi.org/10.1017/qua.2018.46.

Quinn, R.L., 2019. Isotopic equifinality and rethinking the diet of *Australopithecus anamensis*. Am. J. Phys. Anthropol. 169, 403–421. https://doi.org/10.1002/ajpa.23846.

Renne, P.R., WoldeGabriel, G., Hart, W.K., Heiken, G., White, T.D., 1999. Chronostratigraphy of the Miocene–Pliocene Sagantole Formation, Middle Awash Valley, Afar rift, Ethiopia. Geol. Soc. Am. Bull. 111, 869–885. https://doi.org/10.1130/0016-7606(1999)111%3C0869:COTMPS%3E2.3.CO;2.

Robinson, J.R., Rowan, J., Campisano, C.J., Wynn, J.G., Reed, K.E., 2017. Late Pliocene environmental change during the transition from *Australopithecus* to *Homo*. Nat. Ecol. Evol. 1, 0159. https://doi.org/10.1038/s41559-017-0159.

Sahnouni, M., Parés, J.M., Duval, M., Cáceres, I., Harichane, Z., van der Made, J., Pérez-González, A., Abdessadok, S., Kandi, N., Derradji, A., Medig, M., Boulaghraif, K., Semaw, S., 2018. 1.9-million-and 2.4-million-year-old artifacts and stone tool–cutmarked bones from Ain Boucherit, Algeria. Science 362 (6420), 1297–1301. https://doi.org/10.1126/science.aau0008.

Salzmann, U., Haywood, A.M., Lunt, D.J., Valdes, P.J., Hill, D.J., 2008. A new global biome reconstruction and data-model comparison for the Middle Pliocene. Glob. Ecol. Biogeogr. 17, 432–447. https://doi.org/10.1111/j.1466-8238.2008.00381.x.

Saylor, B.Z., Gibert, L., Deino, A., Alene, M., Levin, N.E., Melillo, S.M., Peaple, M.D., Feakins, S.J., Bourel, B., Barboni, D., Novello, A., Sylvestre, F., Mertzman, S.A., Haile-Selassie, Y., 2019. Age and context of mid-Pliocene hominin cranium from Woranso-Mille, Ethiopia. Nature 573 (7773), 220–224. https://doi.org/10.1038/s41586-019-1514-7.

Schuster, M., Duringer, P., Ghienne, J.-F., Roquin, C., Sepulchre, P., Moussa, A., Lebatard, A.-E., Mackaye, H.T., Likius, A., Vignaud, P., Brunet, M., 2009. Chad Basin: paleoenvironments of the Sahara since the late Miocene. C. R. Geoscience 341 (8–9), 603–611. https://doi.org/10.1016/j.crte.2009.04.001.

Senut, B., 2020. *Orrorin tugenensis* et les origines de l'homme: une synthèse. Bull. Acad. Nat. Méd. 204 (3), 258–267. https://doi.org/10.1016/j.banm.2019.12.018.

Shcheglovitova, M., Anderson, R.P., 2013. Estimating optimal complexity for ecological niche models: a jackknife approach for species with small sample sizes. Ecol. Model. 269, 9–17. https://doi.org/10.1016/j.ecolmodel.2013.08.011.

Skonieczny, C., Paillou, P., Bory, A., Bayon, G., Biscara, L., Crosta, X., Eynaud, F., Malaizé, B., Revel, M., Aleman, N., Barusseau, J.-P., Vernet, R., Lopez, S., Grousset, F., 2015. African humid periods triggered the reactivation of a large river system in Western Sahara. Nat. Commun. 6 (1), 1–6. https://doi.org/10.1038/ncomms9751.

Sponheimer, M., 2013. Some ruminations on australopith diets. In: Reed, K.E., Fleagle, J. G., Leakey, R.E. (Eds.), The Paleobiology of *Asustralopithecus*. Springer, Dordrecht, pp. 225–233. https://doi.org/10.1007/978-94-007-5919-0_15.

Su, D.F., Harrison, T., 2008. Ecological implications of the relative rarity of fossil hominins at Laetoli. J. Hum. Evol. 55, 672–681. https://doi.org/10.1016/j.jhevol.2008.07.003.

Sussman, R.W., Hart, D., 2015. Modeling the past: The primatological approach. In: Henke, W., Tattersall, I. (Eds.), Handbook of Paleoanthropology. Springer, Berlin, Heidelberg, pp. 791–815.

Tan, N., Ramstein, G., Dumas, C., Contoux, C., Ladant, J.B., Sepulchre, P., Zhang, Z., De Schepper, S., 2017. Exploring the MIS M2 glaciation occurring during a warm and high atmospheric CO2 Pliocene background climate. Earth Planet. Sci. Lett. 472, 266–276. https://doi.org/10.1016/j.epsl.2017.04.050.

Tan, N., Ladant, J.B., Ramstein, G., Dumas, C., Bachem, P., Jansen, E., 2018. Dynamic Greenland ice sheet driven by pCO_2 variations across the Pliocene Pleistocene transition. Nat. Commun. 9, 4755. https://doi.org/10.1038/s41467-018-07206-w.

Tan, N., Contoux, C., Ramstein, G., Sun, Y., Dumas, C., Sepulchre, P., Guo, Z., 2020. Modeling a modern-like pCO_2 warm period (Marine Isotope Stage KM5c) with two versions of an Institut Pierre Simon Laplace atmosphere–ocean coupled general circulation model. Clim. Past 16, 1–16. https://doi.org/10.5194/cp-16-1-2020.

Uno, K.T., Polissar, P.J., Jackson, K.E., deMenocal, P.B., 2016. Neogene biomarker record of vegetation change in eastern Africa. Proc. Natl. Acad. Sci. U. S. A. 113, 6355–6363. https://doi.org/10.1073/pnas.1521267113.

VanDerWal, J., Shoo, L.P., Graham, C., Williams, S.E., 2009. Selecting pseudo-absence data for presence-only distribution modeling: how far should you stray from what you know? Ecol. Model. 220 (4), 589–594. https://doi.org/10.1016/j.ecolmodel.2008.11.010.

Vignaud, P., Duringer, P., Mackaye, H.T., Likius, A., Blondel, C., Boisserie, J.-R., Bonis, L., Eisenmann, V., Etienne, M.-E., Geraads, D., Guy, F., Lehmann, T., Lihoreau, F., Lopez-Martinez, N., Mourer-Chauviré, C., Otero, O., Rage, J.-C., Schuster, M., Viriot, L., Zazzo, A., Brunet, M., 2002. Geology and palaeontology of the Upper Miocene Toros-Menalla hominid locality. Chad. Nature 418 (6894), 152–155. https://doi.org/10.1038/nature00880.

Ward, C.V., Manthi, F.K., Plavcan, J.M., 2013. New fossils of *Australopithecus anamensis* from Kanapoi, West Turkana, Kenya (2003–2008). J. Hum. Evol. 65, 501–524. https://doi.org/10.1016/j.jhevol.2013.05.006.

Warren, D.L., Seifert, S.N., 2011. Ecological niche modeling in Maxent: the importance of model complexity and the performance of model selection criteria. Ecol. Appl. 21, 335–342. https://doi.org/10.1890/10-1171.1.

White, T.D., Hart, W.K., Walter, R.C., WoldeGabriel, G., Heinzelin, J., Clark, J.D., Asfaw, B., Vrba, E., 1993. New discoveries of Australopithecus at Maka in Ethiopia. Nature 366 (6452), 261–265. https://doi.org/10.1038/366261a0.

White, T.D., Suwa, G., Asfaw, B., 1994. *Australopithecus ramidus*, a new species of early hominid from Aramis, Ethiopia. Nature 371, 306–312. https://doi.org/10.1038/371306a0.

White, T.D., WoldeGabriel, G., Asfaw, B., Ambrose, S., Beyene, Y., Bernor, R.L., Boisserie, J.-R., Currie, B., Gilbert, H., Haile-Selassie, Y., Hart, W.K., Hlusko, L.J., Howell, F.C., Kono, R.T., Lehmann, T., Louchart, A., Lovejoy, C.O., Renne, P.R., Saegusa, H., Vrba, E.S., Wesselman, H., Suwa, G., 2006a. Asa Issie, Aramis and the origin of *Australopithecus*. Nature 440 (7086), 883–889. https://doi.org/10.1038/nature04629.

White, T.D., Howell, F.C., Gilbert, H., 2006b. The earliest *Metridiochoerus* (Artiodactyla: Suidae) from the Usno Formation, Ethiopia. Trans. R. Soc. S. Afr. 61, 75–79. https://doi.org/10.1080/00359190609519955.

White, T.D., Asfaw, B., Beyene, Y., Haile-Selassie, Y., Lovejoy, C.O., Suwa, G., WoldeGabriel, G., 2009. *Ardipithecus ramidus* and the paleobiology of early hominids. Science 326 (5949), 64–86. https://doi.org/10.1126/science.1175802.

WoldeGabriel, G., Ambrose, S.H., Barboni, D., Bonnefille, R., Bremond, L., Currie, B., DeGusta, D., Hart, W.K., Murray, A.M., Renne, P.R., Jolly-Saad, M.C., Stewart, K.M., White, T.D., 2009. The geological, isotopic, botanical, invertebrate, and lower vertebrate surroundings of *Ardipithecus ramidus*. Science 326 (5949). https://doi.org/10.1126/science.1175817, 65–65e5.

Wynn, J.G., Reed, K.E., Sponheimer, M., Kimbel, W.H., Alemseged, Z., Bedaso, Z.K., Campisano, C.J., 2016. Dietary flexibility of *Australopithecus afarensis* in the face of paleoecological change during the middle Pliocene: Faunal evidence from Hadar, Ethiopia. J. Hum. Evol. 99, 93–106. https://doi.org/10.1016/j.jhevol.2016.08.002.

Zhang, R., Yan, Q., Zhang, Z.S., Jiang, D., Otto-Bliesner, B.L., Haywood, A.M., Hill, D.J., Dolan, A.M., Stepanek, C., Lohmann, G., Contoux, C., Bragg, F., Chan, W.-L., Chandler, M.A., Jost, A., Kamae, Y., Abe-Ouchi, A., Ramstein, G., Rosenbloom, N.A., Sohl, L., Ueda, H., 2013. Mid-Pliocene East Asian monsoon climate simulated in the PlioMIP. Clim. Past 9 (5), 2085–2099. https://doi.org/10.5194/cp-9-2085-2013.

Zhang, Z., Li, X., Guo, C., Otterå, O.H., Nisancioglu, K.H., Tan, N., Contoux, C., Ramstein, G., Feng, R., Otto-Bliesner, B.L., Brady, E., Chandan, D., Peltier, W.R., Baatsen, M.L.J., von der Heydt, A.S., Weiffenbach, J.E., Stepanek, C., Lohmann, G., Zhang, Q., Li, Q., Chandler, M.A., Sohl, L.E., Haywood, A.M., Hunter, S.J., Tindall, J. C., Williams, C., Lunt, D.J., Chan, W.-L., Abe-Ouchi, A., 2021. Mid-Pliocene Atlantic Meridional Overturning Circulation simulated in PlioMIP2. Clim. Past 17, 529–543. https://doi.org/10.5194/cp-17-529-2021.